Discover Oncology

Research

Mucinous breast cancer organoids: an in vitro research model

Dongyi Zhao[1] · Shida Zhu[1] · Xue Bai[1] · Xuelu Li[1] · Zuowei Zhao[1]

Received: 9 October 2024 / Accepted: 6 May 2025
Published online: 19 May 2025

Abstract

Background Pure mucinous breast cancer is an uncommon form of cancer characterized by a low metastatic rate and a generally favorable prognosis. However, some patients may experience lymph node metastasis, leading to a worse prognosis. Currently, there is no reliable in vitro model available to effectively address the heterogeneity of pure mucinous breast cancer.

Methods We obtained surgical tumor samples from a 64-year-old Chinese female patient diagnosed with pure mucinous breast cancer to establish patient-derived organoids. Using these organoids, we performed histological staining, drug testing and single-cell RNA-Seq analysis.

Results We accomplished the establishment of a patient-derived mucinous breast cancer organoid model from a Chinese female. Hematoxylin and eosin staining, along with immunohistochemistry, revealed histology and protein expression (ER, PR, HER2 and Ki-67) at early passages similar to the original breast cancer tissue. Single-cell RNA sequencing at passage 7 identified 17 cell clusters, which were assigned to three cell types based on marker genes. This showed that most ER-positive luminal cells had been replaced by ER-negative basal-like cells at passage 7. We tested drug sensitivity to five antitumor drugs at passage 5. The organoids showed the highest sensitivity to Epirubicin and the lowest sensitivity to Carboplatin.

Conclusions This is the first reported case of a mucinous breast cancer organoid. Our experimental results indicate that this model exhibits similar characteristics to the original tissue at early passages. Organoids at early passages could be a promising tool for clinical drug screening and further scientific research.

Keywords Mucinous breast cancer · Organoid · Single-cell RNA-Seq analysis · Heterogeneity

1 Introduction

Mucinous breast cancer is an uncommon form of cancer, representing 1% to 4% of total breast cancer [1, 2]. In 2019, the World Health Organization (WHO) classified mucinous breast cancer (MBC) into two types: pure mucinous breast cancer (PMBC) and mixed mucinous breast cancer (MMBC) [3]. PMBC typically comprises at least 90% mucin

Dongyi Zhao, Shida Zhu, and Xue Bai made equal contributions to this project.

Supplementary Information The online version contains supplementary material available at https://doi.org/10.1007/s12672-025-02586-0.

✉ Xuelu Li, dmulixl@163.com; ✉ Zuowei Zhao, dmuzhaozuowei@163.com; Dongyi Zhao, 357934719@qq.com; Shida Zhu, zsd18845720809@163.com; Xue Bai, 18041165350@163.com | [1]Department of Breast Surgery, The Second Hospital of Dalian Medical University, Dalian 116023, China.

composition, whereas MMBC contains between 30% and 90% mucin composition [4]. PMBC typically manifests as a homogeneous mass of tumor cells surrounded by plentiful extracellular mucin, and it has a much better prognosis compared to invasive ductal carcinoma [5]. PMBC typically expresses estrogen receptor (ER) and progesterone receptor (PR), but does not have amplification of Human Epidermal Growth Factor Receptor 2 (HER2) [6]. According to a retrospective analysis involving 11,400 cases of pure mucinous breast cancer, 86% exhibited no nodal or distant metastases, 12% showed regional nodal involvement, and 2% presented with distant metastases [2]. Cox multivariate analysis revealed that lymph node condition is the key prognostic indicator, with the survival curve of node-negative patients markedly differing from that of node-positive patients [2, 5]. This finding was confirmed by Cao et al. [2, 5]. However, there is currently no reliable model to elucidate mucinous breast cancer.

Human patient-derived organoids (PDOs) are emerging three-dimensional models that closely simulate the biological characteristics of the original tissue [7, 8]. PDOs have been utilized in multiple breast cancer-related studies, covering various breast cancer subtypes [9–12] and different distant metastasis organs of breast cancer [13, 14]. Furthermore, high-fidelity breast cancer organoids are crucial tools for tailoring treatment strategies for patients with rare breast cancer types. Our team has successfully established patient-derived organoids for various uncommon breast diseases [15–17]. This study reports a case of a 64-year-old Chinese female patient diagnosed with pure mucinous breast cancer (PMBC) accompanied by axillary lymph node metastasis. We established a patient-derived mucinous breast cancer organoid model. This is also the first instance of patient-derived organoids from PMBC.

2 Materials and methods

2.1 Organoid culture

Following the surgical procedure, the collected specimens are promptly transported to the laboratory under controlled conditions, preserved in a cold culture medium. Once in the lab, the specimens are meticulously cut into smaller fragments to facilitate the subsequent processing steps. Prior to enzymatic processing, the specimen fragments undergo rigorous washing with advanced DMEM/F12 medium sourced from Sigma (Saint Louis, MO, USA). Subsequently, collagenase IV, also sourced from Sigma and used at a concentration of 1.5 mg/mL, is employed for the digestion of the tissue fragments. After 2 h of dissociation, the digested cell suspension was suspended in ADDF+++ solution and centrifuged. The pellet was then suspended in Matrigel and culture medium. 40 µL mixture of suspension droplets and medium was added to each well of a 24-well suspension plate. After completion of gelation, 400 µL of growth medium was added to each well. To maintain the health and viability of the organoid cultures, the growth medium is replaced every 3 days. Additionally, the organoids are passaged periodically, typically every 2–3 weeks, based on an assessment of their size and morphological characteristics. Passaging is achieved through a digestion process using TrypLE Express (Invitrogen, Carlsbad, CA, USA) at 37 °C for 20 min, combined with gentle mechanical pipetting to achieve complete dissociation of the cells. During the digestion phase, the progress is carefully monitored under a microscope to ensure that the cells are appropriately dissociated. The digestion process is terminated when approximately 90–95% of the cells in the microscopic field of view appear as single, viable cells. Following digestion, ADDF+++ solution is once again added, and the cell suspension is centrifuged at 1000 rpm to collect the cell pellet. The organoids are then passaged at a 1:2 ratio to ensure that sufficient numbers of cells are available for continued culture and research. In summary, this detailed protocol for organoid culture follows a rigorous and precise methodology, building on established techniques and principles [15–17].

2.2 Immunohistochemistry

The collected droplets were carefully transferred to Collagen (Biocoat, Corning, NY, USA), preserving their 3D structure. After fixation with 4% paraformaldehyde, the collagen underwent dehydration, clearing with dimethylbenzene, and paraffin embedding. The organoids were then sectioned into 5-µm slices and stained using an Immunohistochemistry Kit and DAB Kit, adhering strictly to the manufacturer's guidelines.

The following primary antibodies were utilized: anti-estrogen receptor alpha (1:50, Abcam ab16660), anti-progesterone receptor (1:100, Abcam ab63605), anti-ErbB2/HER2 (1:1000, Abcam ab134182), and anti-Ki67 (1:200, Abcam ab16667), sourced

from Abcam (Cambridge, MA, UK). Antigen retrieval involved microwave heating in sodium citrate solution at 95 °C for 20 min. Immunohistochemistry procedures adhered to established methods [15–17], utilizing DAB kits from Zhongshan Golden Bridge Biotechnology Co.

2.3 Drug screen

Mucinous breast cancer organoids were dissociated into single cells and cultured for seven days prior to experimentation. The resultant cell pellet was resuspended in growth medium containing 5% Matrigel to achieve a concentration of about 70 organoids per microliter. A 384-well assay plate (Nest, Wuxi, Jiangsu, China) was pre-coated with Matrigel, and each well received 30 µL of the prepared suspension, having been previously primed with 10 µL of Matrigel.

Subsequently, a range of concentrations (0, 0.001 µM, 0.01 µM, 0.1 µM, 1 µM, 10 µM, 20 µM, 50 µM) of Hydroxytamoxifen, Fulvestrant, Palbociclib, Epirubicin, and Carboplatin were introduced, along with DMSO/DMF controls. The drugs—Hydroxytamoxifen (HY-16950), Fulvestrant (HY-13636), Palbociclib (HY-50767), Epirubicin (HY-13624), and Carboplatin (HY-17393)—were sourced from MedChemExpress.

After five days of incubation, 25 µL of CellTiter-Glo 3D reagent (Promega, Madison, WI, USA) was applied to each well. The plate was incubated at room temperature for 30 min before analysis using a SpectraMax microplate reader. The resulting data was processed with GraphPad Prism 6, and IC50 values were determined through manual calculation.

2.4 Single-cell RNA sequencing

The organoids were dissociated into single cells using established protocols. The cells were spun down at 1000 rpm for 5 min and resuspended in 1 mL of PBS (Gibco, NY, USA). After manual counting, the cell concentration was adjusted to 1×10^5 cells per mL in PBS. Subsequently, the cells were captured using microfluidic chips from Singleron Biotechnologies (Jiangsu, China) for library construction and sequencing, also performed by Singleron Biotechnologies.

For sequencing data processing, a substantial number of raw reads—totaling 665,271,396—were meticulously analyzed using the CeleScope v2.1.1 pipeline provided by Singleron Biotechnologies (Jiangsu, China). Scanpy was employed for quality control, dimensionality reduction, and clustering in our analysis [18, 19]. Rigorous filtering criteria were applied to the cells: those with fewer than 200 detected genes, those within the top 2% of genes or UMI counts, and those with mitochondrial content exceeding 5% were excluded. Furthermore, genes expressed in fewer than five cells were also omitted. Following this meticulous filtering process, 14,505 cells remained for further exploration. The raw count matrix was normalized according to the total counts per cell and underwent log-transformation. Utilizing the Seurat method (flavor = 'seurat'), the top 2000 highly variable genes were meticulously selected and subjected to Principal Component Analysis (PCA) [20]. For clustering and dimensionality reduction, the first 20 principal components were chosen, with the resolution parameter set to 1.2, ultimately yielding 17 distinct clusters. To visualize these clusters, Uniform Manifold Approximation and Projection (UMAP) was employed, providing a comprehensive and intuitive representation of our data [21].

Cell identity was established through hypergeometric tests (HGT) on extracted gene signatures, enabling the identification of characteristic gene sets for each cell [22]. Cluster annotation was conducted using both automated and manual methods within the SynEcoSys database (Singleron Biotechnologies, Jiangsu, China). Marker gene expression for each cell type was visualized using dot plots generated by Seurat functions [23].

3 Results

3.1 Case report

During a routine physical examination, a 64-year-old woman was found to have a hard lump in her left breast. The patient has a history of endometrial cancer, and her sister has a history of breast cancer. Physical examination revealed an ill-defined, immobile mass measuring 4 cm in diameter in the left breast. The CT scan showed an irregular mass with indistinct borders in the left breast (Fig. 1a). Following an ultrasound-guided core needle biopsy of the lesion, the results indicated that the tumor was an adenocarcinoma, with the tumor nests observed floating in a mucinous lake. The patient subsequently underwent a modified radical mastectomy. Postoperative pathological analysis confirmed the lesion as pure mucinous breast cancer (PMBC), with one lymph node showing metastasis. The

immunohistochemistry (IHC) results confirmed that estrogen receptor (ER) and progesterone receptor (PR) staining were positive (Strongly Positive 90%), HER2 (1+) and Ki67 (Positive 10%) (Fig. 1c).

3.2 Establishing patient-derived PMBC organoids

We obtained the surgical fresh mucinous breast cancer tissue (Fig. 1a). The organoid culture method used was identical to the one employed in our previous study [15–17]. We documented the developmental progression of the organoids on passage 3, 6, 9, 12, and conducted multiple passages (Fig. 1b). After a long-term culture, the morphology and growth rate of mucinous breast cancer organoids remained approximately similar compared to the initial culture period (Fig. 1b).

3.3 The PMBC organoids retained the characteristics of the original PMBC

To evaluate the fidelity of the organoid model in replicating the original mucinous breast cancer tissue, we performed H&E staining and IHC analyses on both the organoid and the original cancer tissue sections. Vesicular structures akin to those found in the original cancer tissue can be observed in both light microscopy and hematoxylin and eosin staining (Fig. 1c). Furthermore, IHC results indicated the positive expression of estrogen receptor (ER) and progesterone receptor (PR), along with weak positive expression of human epidermal growth factor receptor 2 (HER2) and Ki-67 (Fig. 1c).

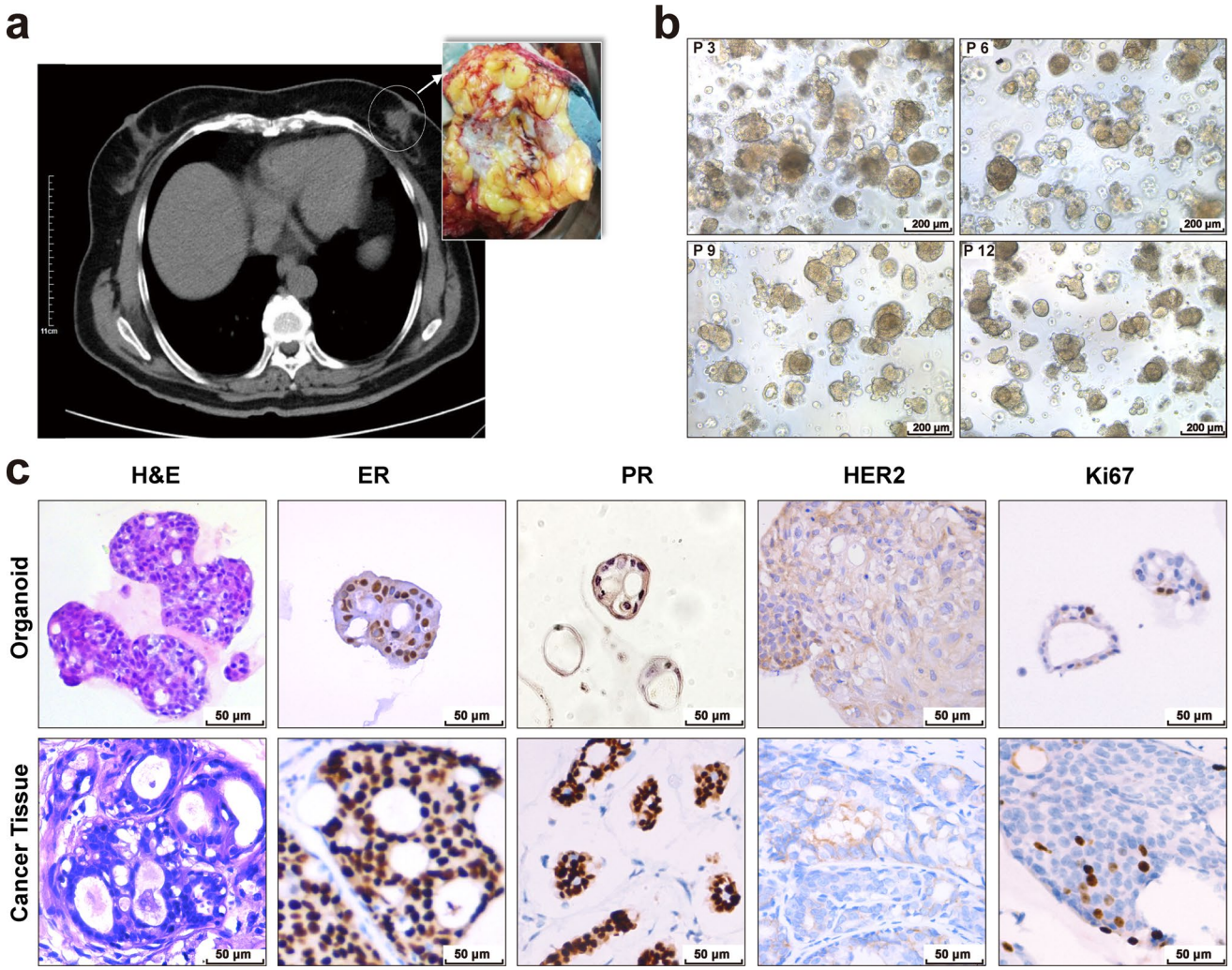

Fig. 1 Establishing patient-derived PMBC organoids. **a** The patient's CT scan revealed an irregular shadow in the left breast, confirmed as cancerous tissue following modified radical mastectomy. **b** Representative images of the third, sixth, ninth and twelfth generations on the tenth day of incubation. **c** Representative images of H&E and IHC of third-generation organoids. *ER* estrogen receptor, *PR* progesterone receptor, *HER2* human epidermal growth factor receptor-2, *Ki-67* Antigen Ki67

Subsequent cryopreservation did not induce significant changes in the H&E staining of the PMBC organoids compared to the unfrozen samples (Fig. 2). ER/PR-positive expression was retained in organoids after freezing, but decreased compared to the original tissue and third-generation organoids (Figs. 1c and 2). In conclusion, these findings indicate that the structural characteristics and molecular biomarker expressions of the PMBC organoids resemble those of the original PMBC tissue.

3.4 Optimizing treatment strategy based on PMBC organoid model

We utilized the PMBC organoids to perform drug sensitivity testing on five common antitumor drugs. The results showed that the PMBC organoids exhibited the highest sensitivity to Epirubicin (IC50 = 0.020 μmol/L), followed by Palbociclib (IC50 = 0.36 μmol/L), Fulvestrant (IC50 = 4.4 μmol/L), and Hydroxytamoxifen (IC50 = 4.4 μmol/L), with the lowest sensitivity to Carboplatin (IC50 = 51 μmol/L) (Fig. 3). Together, this PMBC organoids exhibit heterogeneity in response to different types of medicine.

3.5 Single-cell RNA sequencing of mucinous breast cancer organoid

We performed single-cell RNA sequencing analysis on the 7th generation of the PMBC organoid. Clustering of single-cell gene expression data revealed 17 distinct clusters with varying gene expression characteristics (Supplementary material 1). The t-SNE was employed for dimensionality reduction and subtype representation (Fig. 4a). We annotated the cells based on the marker genes of each cell cluster, and eventually, these 17 cell clusters were classified into three types of cells: basal cells, luminal epithelial cells, and proliferating basal cells. We projected these three types of cells onto a t-SNE plot for visualization and represented the percentage of different cell types in the total cell population with a bar chart (Fig. 4b). Almost all cells in cluster 12 are defined as proliferating luminal epithelial cells. The abbreviations and corresponding marker genes for these three cell types are listed here (Supplementary material 2). Next, we selected the top 15 differential genes from each of the three types of cells, making a total of 45 differential genes for comparison, and displayed them using a dot plot (Fig. 4c). Finally, we performed single-cell detection of common breast cancer genes and projected the detection results of each original gene onto the t-SNE dimensionality reduction map. This clearly reflects the expression levels of marker genes within each cell cluster. We present the expression of three genes (ESR1, PGR, and ERBB2) across each cell cluster. The results are consistent with the aforementioned IHC results, showing that ER/PR receptors are expressed in cells annotated as Luminal epithelial cells, while ERBB2 is expressed at low levels in these cells (Fig. 4d). In summary, these results indicate that there is heterogeneity among PMBC organoid.

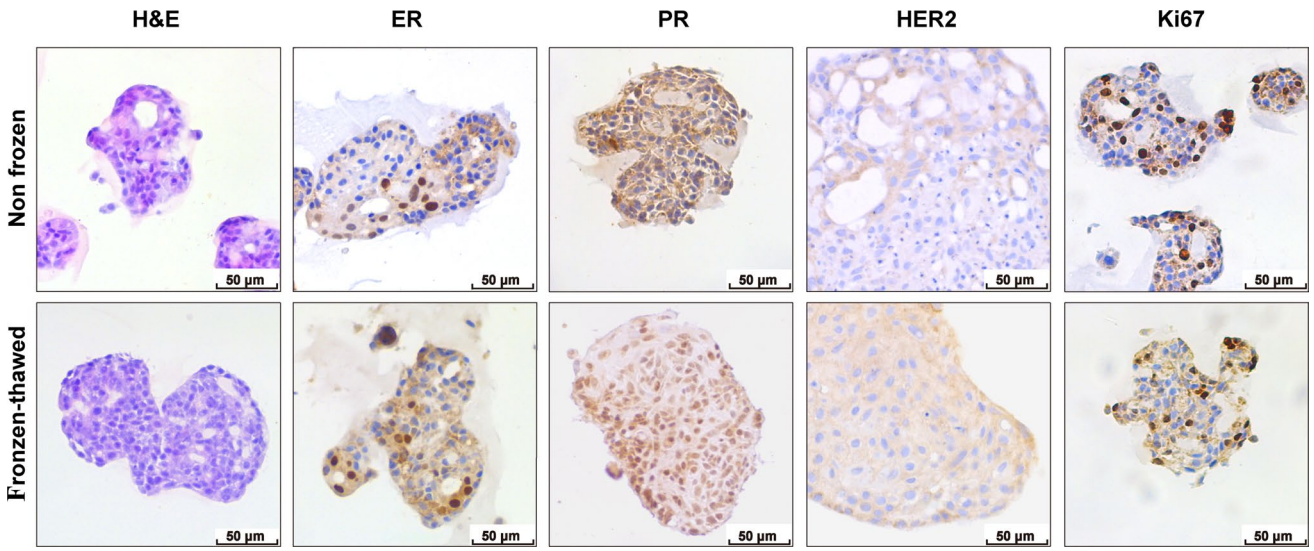

Fig. 2 The PMBC organoids exhibit stability. Representative images of H&E and IHC for fifth-generation organoids before and after cryopreservation

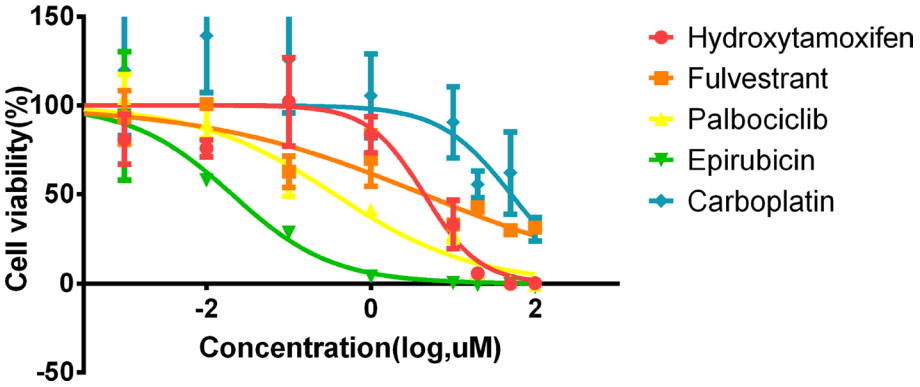

Fig. 3 Drug sensitivity of the PMBC organoids. The x-axis represents drug concentration, the y-axis represents cell viability, and different colors represent different drugs. The organoids of fifth passage were treated, the duration of drug exposure was 5 days (n = 3 wells per condition, n = 3 separate experiments). Error bars represent standard deviation. The IC50 is the half-maximal inhibitory concentration for different drugs

4 Discussion

We developed a mucinous breast cancer organoid model to mimic this MBC tumor. Through H&E staining and immunohistochemistry, we confirmed that the PMBC organoids displayed similar morphological features and molecular

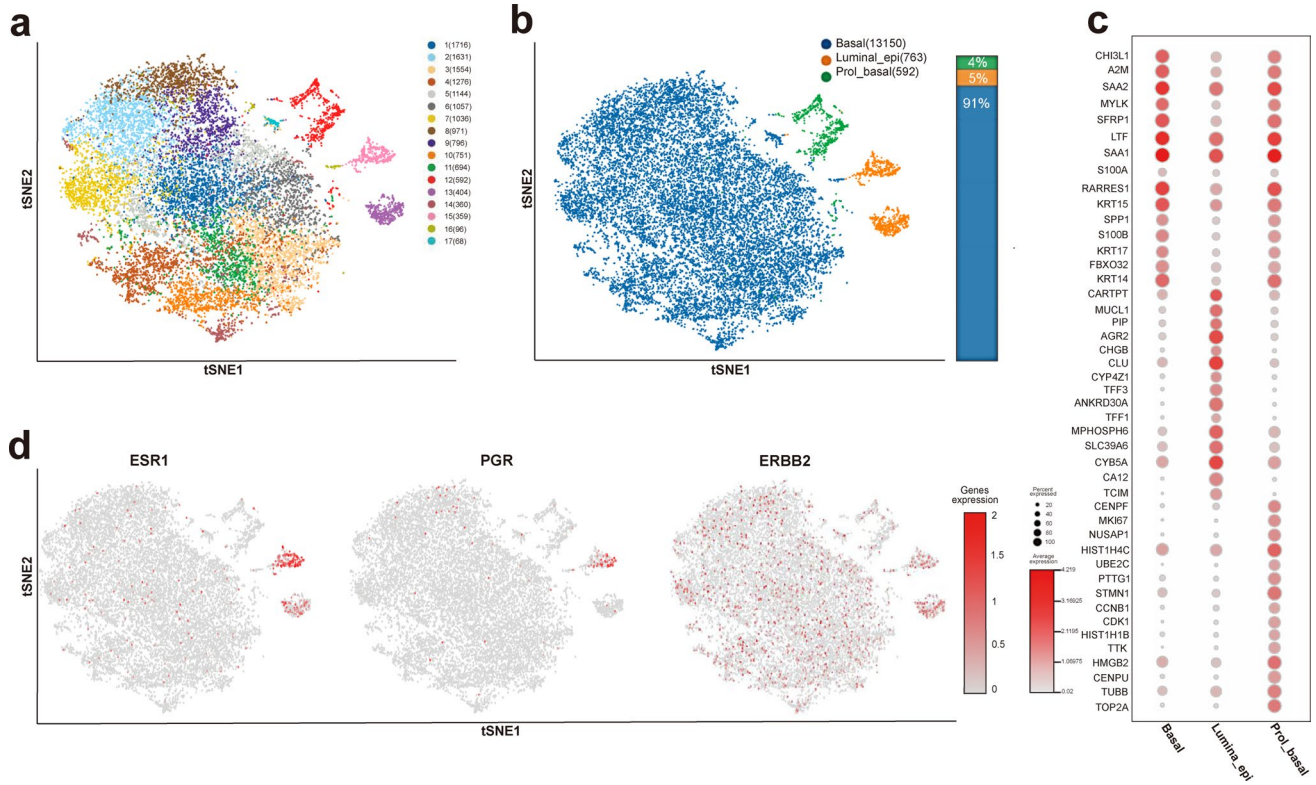

Fig. 4 Single-cell RNA sequencing analysis of the PMBC organoids. Single-cell RNA sequencing was performed on the 7th generation organoids. **a** The t-SNE visualization of all cells in PMBC organoid sample, with clusters color-coded. The number in brackets is the cell number of the cluster. **b** Cells are annotated into three main types, with different colors representing different cell types. The bar chart shows the proportion of each cell type in the total cell count. Basal, Basal cells; Lumina epi, Luminal epithelial cells; Pro basal, Proliferating basal cells. **c** Dot plot of marker genes display. The FindAllMarkers module of Seurat software was used to identify marker genes for all clusters. The dot plot is horizontally represented by cluster ID and vertically by gene ID. Larger circles indicate a higher proportion of gene expression in the cluster, and redder colors indicate higher average expression levels of the gene. **d** The expression values of ESR1, PGR, and ERBB2 genes are mapped onto the t-SNE plot to show their expression levels in each cell. Darker red indicates higher expression

biomarkers as the original PMBC tissue. As far as we know, this is the first report on creating patient-derived organoids from PMBC.

We conducted drug sensitivity testing and single-cell RNA sequencing on the PMBC organoids. Based on the results of drug sensitivity experiments, the PMBC PDOs displayed varying sensitivities to the different drugs, suggesting a unique reaction to each regimen. Heterogeneity of response to drugs suggested the potential of PMBC PDOs as models for drug sensitivity testing. The single-cell RNA sequencing results confirmed that the PMBC organoids exhibit heterogeneity, providing a valuable model for scientific research and an innovative approach for studying mucinous breast cancer. Based on the results of IHC and scRNAseq, these organoids retain similar feature of the primary tumor, however, the intensity of ER expression and the percentage of positive cells decreased gradually. A large portion of ER-positive cells did not retain their high-level expression. We performed single-cell RNA sequencing of seventh-generation organoids and observed a partial loss of ER/PR, similar to that observed by other laboratories [24]. It suggests that maintaining hormone receptor expression at a high level is difficult for organoids under the selective pressure of the external microenvironment. With an increase in passage number, the rapidly expanding population of organoids, like the Basal-Like subtype, is progressively chosen and grown. Additionally, previous lineage tracing studies have revealed that early mammary organoids preserve the pluripotency of mammary stem cells, exhibiting the capacity to differentiate into both luminal and basal cell lineages concurrently [25]. Conversely, cells that were labeled at later stages predominantly generated basal cell lineages. Improving long-term reliability is shown to be a significant and rewarding endeavor in this discipline by these phenomena.

There are also some limitations to our study, we identified only the 3 cell types mentioned above and did not include the stromal cells, such as immune-related cells and so on. Due to the limited amount of tumor tissue available, we only had enough tissue to attempt organoids cultures and pathology experiments. Therefore, we did not conduct single-cell RNA sequencing on the primary tumor tissue.

Author contributions Dongyi Zhao was responsible for collecting clinical samples, all experimental operations, and participated in writing the manuscript and creating the figures. Shida Zhu wrote the manuscript and created the figures. Xue Bai organized and analyzed the single-cell RNA sequencing data. Xuelu Li and Zuowei Zhao conceived and designed the study and were responsible for manuscript review.

Funding This research received funding from the National Natural Science Foundation of China (82203800, 82072934), Natural Science Foundation of Liaoning Province (2023-MSLH-022), Educational Reform Project of Dalian Medical University (DYLX22014) and 1+X program of the Second Hospital of Dalian Medical University (2022QNJXJYFH01, 2022LCYJYB03, 2022JXGGYJ011).

Data availability Data is provided within the manuscript or supplementary information files.

Declarations

Ethics approval and consent to participate Approval was obtained from the Ethics Committee of The Second Hospital of Dalian Medical University. The methods employed in this research comply with the principles of the Declaration of Helsinki. Informed consent was secured from each participant involved in the study.

Consent for publication Patient signed informed consent regarding publishing her data and photographs.

Competing interests The authors declare no competing interests.

References

1. Park S, Koo J, Kim JH, Yang WI, Park BW, Lee KS. Clinicopathological characteristics of mucinous carcinoma of the breast in Korea: comparison with invasive ductal carcinoma-not otherwise specified. J Korean Med Sci. 2010;25(3):361–8.
2. Di Saverio S, Gutierrez J, Avisar E. A retrospective review with long term follow up of 11,400 cases of pure mucinous breast carcinoma. Breast Cancer Res Treat. 2008;111(3):541–7.
3. Tan PH, Ellis I, Allison K, Brogi E, Fox SB, Lakhani S, Lazar AJ, Morris EA, Sahin A, Salgado R, et al. The 2019 World Health Organization classification of tumours of the breast. Histopathology. 2020;77(2):181–5.

4. Marrazzo E, Frusone F, Milana F, Sagona A, Gatzemeier W, Barbieri E, Bottini A, Canavese G, Rubino AO, Eboli MG, et al. Mucinous breast cancer: a narrative review of the literature and a retrospective tertiary single-centre analysis. Breast. 2020;49:87–92.
5. Cao AY, He M, Liu ZB, Di GH, Wu J, Lu JS, Liu GY, Shen ZZ, Shao ZM. Outcome of pure mucinous breast carcinoma compared to infiltrating ductal carcinoma: a population-based study from China. Ann Surg Oncol. 2012;19(9):3019–27.
6. Nguyen B, Veys I, Leduc S, Bareche Y, Majjaj S, Brown DN, Boeckx B, Lambrechts D, Sotiriou C, Larsimont D, et al. Genomic, transcriptomic, epigenetic, and immune profiling of mucinous breast cancer. J Natl Cancer Inst. 2019;111(7):742–6.
7. Guillen KP, Fujita M, Butterfield AJ, Scherer SD, Bailey MH, Chu Z, DeRose YS, Zhao L, Cortes-Sanchez E, Yang CH, et al. A human breast cancer-derived xenograft and organoid platform for drug discovery and precision oncology. Nat Cancer. 2022;3(2):232–50.
8. Huang C, Jin H. Progress and perspective of organoid technology in breast cancer research. Chin Med J (Engl). 2024;137(18):2157–68.
9. Bhatia S, Kramer M, Russo S, Naik P, Arun G, Brophy K, Andrews P, Fan C, Perou CM, Preall J, et al. Patient-derived triple-negative breast cancer organoids provide robust model systems that recapitulate tumor intrinsic characteristics. Cancer Res. 2022;82(7):1174–92.
10. Pan B, Li X, Zhao D, Li N, Wang K, Li M, Zhao Z. Optimizing individualized treatment strategy based on breast cancer organoid model. Clin Transl Med. 2021;11(4): e380.
11. Mo H, Liu X, Xue Y, Chen H, Guo S, Li Z, Wang S, Li C, Han J, Fu M, et al. S6K1 amplification confers innate resistance to CDK4/6 inhibitors through activating c-Myc pathway in patients with estrogen receptor-positive breast cancer. Mol Cancer. 2022;21(1):171.
12. Zou Y, Zheng S, Xie X, Ye F, Hu X, Tian Z, Yan SM, Yang L, Kong Y, Tang Y, et al. N6-methyladenosine regulated FGFR4 attenuates ferroptotic cell death in recalcitrant HER2-positive breast cancer. Nat Commun. 2022;13(1):2672.
13. Ding K, Chen F, Priedigkeit N, Brown DD, Weiss K, Watters R, Levine KM, Heim T, Li W, Hooda J, et al. Single cell heterogeneity and evolution of breast cancer bone metastasis and organoids reveals therapeutic targets for precision medicine. Ann Oncol. 2022;33(10):1085–8.
14. Onder CE, Ziegler TJ, Becker R, Brucker SY, Hartkopf AD, Engler T, Koch A. Advancing cancer therapy predictions with patient-derived organoid models of metastatic breast cancer. Cancers (Basel). 2023;15(14):3602.
15. Pan B, Zhao D, Liu Y, Li N, Song C, Li N, Li X, Li M, Zhao Z. Establishment and characterization of breast cancer organoids from a patient with mammary Paget's disease. Cancer Cell Int. 2020;20:365.
16. Li X, Pan B, Song X, Li N, Zhao D, Li M, Zhao Z. Breast cancer organoids from a patient with giant papillary carcinoma as a high-fidelity model. Cancer Cell Int. 2020;20:86.
17. Pan B, Zhao D, Liu Y, Li N, Song C, Li N, Li X, Zhao Z. Breast cancer organoids from malignant pleural effusion-derived tumor cells as an individualized medicine platform. In Vitro Cell Dev Biol Anim. 2021;57(5):510–8.
18. Satija R, Farrell JA, Gennert D, Schier AF, Regev A. Spatial reconstruction of single-cell gene expression data. Nat Biotechnol. 2015;33(5):495–502.
19. Wolf FA, Angerer P, Theis FJ. SCANPY: large-scale single-cell gene expression data analysis. Genome Biol. 2018;19(1):15.
20. Groth D, Hartmann S, Klie S, Selbig J. Principal components analysis. Methods Mol Biol. 2013;930:527–47.
21. McInnes L, Healy J, Melville J. Umap: Uniform manifold approximation and projection for dimension reduction. 2018. arXiv preprint arXiv:18020342.
22. Wang Y. Hypergeometric distribution. In: Dubitzky W, Wolkenhauer O, Cho K-H, Yokota H, editors. Encyclopedia of systems biology. New York, NY: Springer; 2013. p. 929–30.
23. Hao Y, Hao S, Andersen-Nissen E, Mauck WM III, Zheng S, Butler A, Lee MJ, Wilk AJ, Darby C, Zager M, et al. Integrated analysis of multimodal single-cell data. Cell. 2021;184(13):3573-3587.e3529.
24. Campaner E, Zannini A, Santorsola M, Bonazza D, Bottin C, Cancila V, Tripodo C, Bortul M, Zanconati F, Schoeftner S, et al. Breast cancer organoids model patient-specific response to drug treatment. Cancers (Basel). 2020;12(12):3869.
25. Yuan L, Xie S, Bai H, Liu X, Cai P, Lu J, Wang C, Lin Z, Li S, Guo Y, et al. Reconstruction of dynamic mammary mini gland in vitro for normal physiology and oncogenesis. Nat Methods. 2023;20(12):2021–33.